PROCEEDINGS OF SCIENCE

Performance of the ATLAS Tile Calorimeter

Stanislav Poláček* **on behalf of the ATLAS Collaboration**

Institute of Particle and Nuclear Physics, Faculty of Mathematics and Physics, Charles University, Prague, Czech Republic

E-mail: stanislav.polacek@cern.ch

The Tile Calorimeter (TileCal) is a hadron calorimeter covering the central region of the ATLAS experiment. It provides important information for the reconstruction of hadrons, jets, hadronic decays of tau leptons, missing transverse energy, and assists in muon identification. The light produced by the passage of charged particles through the scintillating tiles acting as the active material sandwiched between slabs of steel absorber is collected by 9852 photomultipliers. Each stage of the signal production from scintillation light to the signal reconstruction is monitored and calibrated.

The data collected during the LHC Run-2 were used for detailed analyses of the TileCal performance. The effects of prolonged exposure to intense radiation on the TileCal response have been studied. The understanding of the aging of the detector components is crucial concerning the Run-3 and HL-LHC. High-momentum isolated muons have been used to study and validate the electromagnetic scale, while the hadronic response has been probed with isolated hadrons. The calorimeter time resolution has been studied with multi-jet events.

A summary of the performance results including the calibration, stability, absolute energy scale, uniformity, time resolution, and aging of the scintillating tiles and wave-length-shifting fibers will be presented. The first results using the LHC Run-3 data will also be shown.

Corfu Summer Institute 2023 "School and Workshops on Elementary Particle Physics and Gravity" (CORFU2023)
23 April – 6 May, and 27 August – 1 October, 2023
Corfu, Greece

*Speaker

PoS(CORFU2023)020

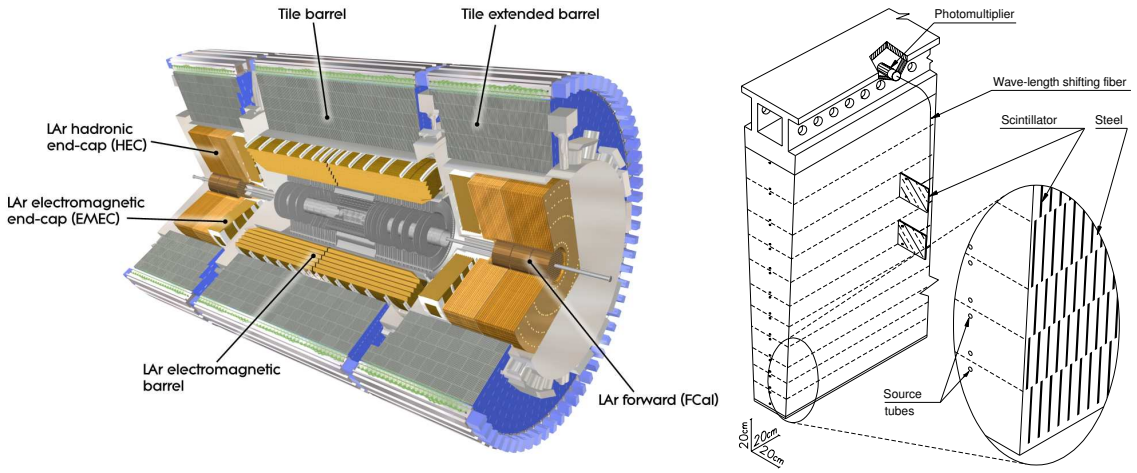

(a) **(b)**

Figure 1: (a) Calorimeter system of the ATLAS experiment [1]. (b) Module of the Tile Calorimeter [1].

1. Tile Calorimeter

The Tile Calorimeter (TileCal) is the central hadronic calorimeter of the ATLAS experiment [1] at the Large Hadron Collider (LHC) [2] at CERN. TileCal plays a major role in the identification of hadronic jets and the measurement of their energy and direction of travel. It also contributes to the missing transverse energy reconstruction, ATLAS trigger systems, and muon identification.

TileCal is a sampling calorimeter made of alternating layers of steel absorber and plastic scintillators [3]. It consists of one central long barrel and two extended barrels (Figure 1a) and covers the pseudorapidity[1] range of $|\eta| < 1.7$. In the azimuthal plane (with respect to the beam axis), each barrel is divided into 64 modules (Figure 1b). Each module consists of 11 rows of the scintillator tiles. Light from the scintillators is collected by wavelength-shifting (WLS) fibers and consequently transmitted to the photomultiplier tubes (PMTs). In each module, groupings of WLS fibers to the same PMTs (readout channels) define the TileCal readout cells, which are divided into three radial layers—A, BC, and D in the long barrel and A, B, and D in the extended barrels (Figure 2). In total, there are 9852 readout channels and 5182 cells, where the majority of cells are read out by two PMTs.

2. Signal reconstruction

The PMT signal is shaped to have a constant width so that the amplitude is proportional to the integral of the signal (and therefore the total collected electrical charge). Then, the shaped signal is divided into two branches called high gain (HG) and low gain (LG) where it is amplified with a

[1]ATLAS uses a right-handed coordinate system with its origin at the nominal interaction point (IP) in the center of the detector and the z-axis along the beam pipe. The x-axis points from the IP to the center of the LHC ring, and the y-axis points upwards. Polar coordinates (r, ϕ) are used in the transverse plane, ϕ being the azimuthal angle around the z-axis. The pseudorapidity is defined in terms of the polar angle θ as $\eta = -\ln\tan(\theta/2)$ and is equal to the rapidity $y = \frac{1}{2}\ln\left(\frac{E+p_z c}{E-p_z c}\right)$ in the relativistic limit. Angular distance is measured in units of $\Delta R \equiv \sqrt{(\Delta y)^2 + (\Delta\phi)^2}$.

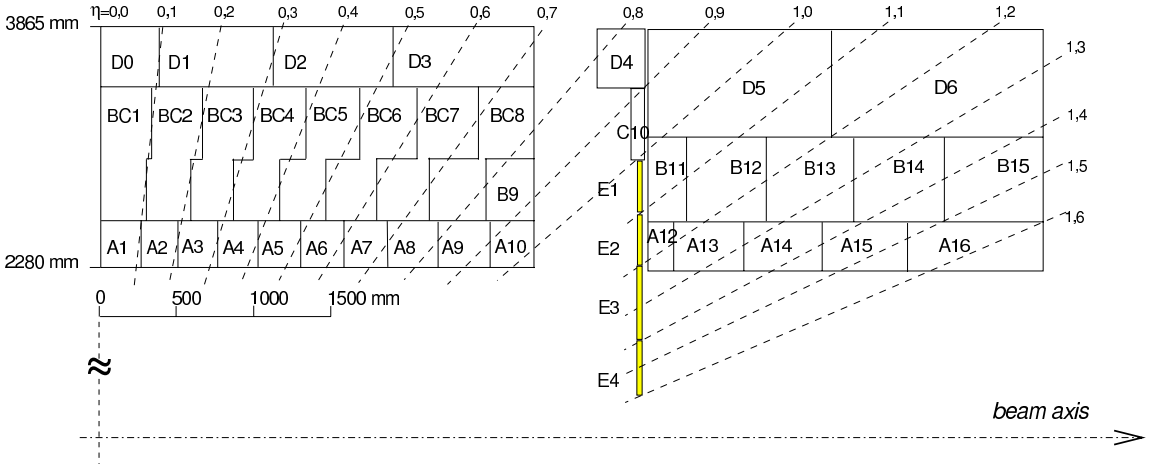

Figure 2: Readout cells of the Tile Calorimeter displayed in half of a module of the long barrel and a module of the extended barrel [4].

relative gain ratio of 64:1. Both HG and LG signals are then sampled every 25 ns using a 10-bit analog-to-digital converters (ADC) producing seven amplitude measurements centered around the expected pulse peak.

The optimal filtering (OF) algorithm [5] is used to reconstruct the signal parameters from the seven measured samples S_i:

$$A = \sum_{i=1}^{7} a_i \cdot S_i, \qquad t = \frac{1}{A} \sum_{i=1}^{7} b_i \cdot S_i, \qquad P = \sum_{i=1}^{7} c_i \cdot S_i, \tag{1}$$

where A is the signal amplitude, t is the time phase relative to the expected signal peak, P is the pedestal, and a_i, b_i, and c_i are constants derived (separately for HG and LG) using the precise shape of the pulse.

The pulse amplitude A from Equation (1) is reconstructed in ADC counts and converted to the channel energy E_{channel} in GeV using constants C_{Cs}, C_{laser}, C_{MB}, and $C_{\text{ADC}\to\text{pC}}$ obtained with TileCal calibration systems (more in Section 3) and constant $C_{\text{pC}\to\text{GeV}}$ measured using electron beams during test beams [6, 7]:

$$E_{\text{channel}}[\text{GeV}] = \frac{A[\text{ADC}]}{C_{\text{Cs}} \cdot C_{\text{laser}} \cdot C_{\text{MB}} \cdot C_{\text{ADC}\to\text{pC}} \cdot C_{\text{pC}\to\text{GeV}}}. \tag{2}$$

3. Calibration and monitoring

Multiple calibration systems are used to calibrate and monitor different steps of the signal reconstruction chain (Figure 3) so that the response of the calorimeter is kept stable and uniform across all its cells.

3.1 Cesium

The cesium calibration system uses capsules with ^{137}Cs γ-radiation source. The capsules are moved through pipes passing all of the calorimeter scintillator tiles using a hydraulic system.

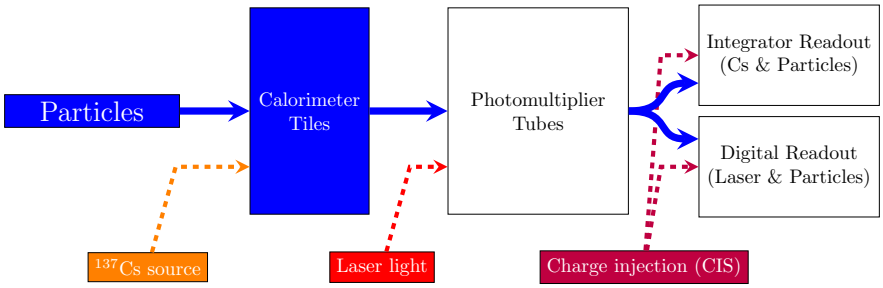

Figure 3: TileCal calibration systems—cesium, laser, and charge injection [6].

The signal is read out by a dedicated integrator system. Since the cesium source illuminates the calorimeter tiles, it monitors all optics components and PMTs. The deviation from the expected response to the cesium source (Figure 4a) is caused by the degradation of scintillator tiles and WLS fibers and by the gain variation of PMTs. The effect is the largest in the innermost radial layer (layer A) of the calorimeter cells due to higher radiation exposure. To obtain a uniform calorimeter response, the constant C_{Cs} from Equation (2) is introduced in each channel. The precision of this system is approximately 0.3% in typical calorimeter cells [6].

3.2 Laser

The laser calibration system uses laser light pulses that are distributed by optics fibers to the photocathodes of all of the PMTs. It is used to monitor the PMT gain stability. Variations in each channel (Figure 4b) are corrected using the calibration constant C_{laser} from Equation (2). The precision of this method is approximately at the level of 0.5% [6, 8]. The laser system is also used to monitor timing in all channels (more in Section 3.6).

3.3 Charge injection

The charge injection system (CIS) injects a signal with a well-defined charge to the readout electronics of all channels. The charge magnitude is varied to cover the whole dynamic range of ADCs of both gains. CIS is used to measure the conversion factor $C_{\mathrm{ADC}\to\mathrm{pC}}$ (Figure 5a) from Equation (2) and to monitor the stability of electronics and the response of ADCs. The precision of this system is approximately 0.7% [6].

3.4 Minimum bias

The minimum bias (MB) system integrates signal created by MB inelastic *pp* interactions at LHC using the integrator readout shared with the cesium system (Section 3.1). The MB current in PMTs is proportional to the instantaneous luminosity and allows for monitoring of the response of the whole optics chain over time (Figure 5b), validation of the response changes observed by the cesium system, and calibration of special cells inaccessible by the ^{137}Cs source. The calibration constant C_{MB} from Equation (2) correcting the response deviation is applied during the reprocessing of the data [6].

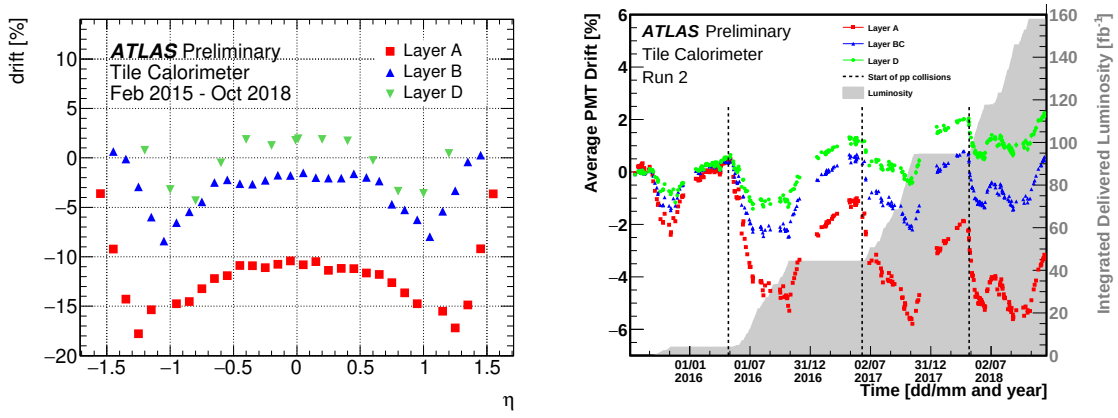

(a) **(b)**

Figure 4: (a) The down-drift of the response to the ^{137}Cs source as a function of pseudorapidity η between the start of Run-2 and the end of Run-2 *pp* collisions and (b) variation of the response to the laser signal during Run-2 in three radial layers of the calorimeter [4]. The integrated luminosity delivered by LHC is plotted in grey.

3.5 Combined calibration and aging

Using the methods mentioned above, the response variation of all optical components and PMTs can be monitored. During the LHC collision periods, the response down-drift is observed (Figure 5b) due to the degradation of scintillators, WLS fibers, and PMTs, which is caused by irradiation of the components. During the periods without collisions, components partially recover and the response up-drift is observed.

Since MB and Cs systems monitor both optical components and PMTs, and laser system monitors just PMTs (bypassing the scintillators and WLS fibers), the difference between calorimeter response to the laser and MB or Cs can be used to study the aging of the calorimeter optical components. The response of the most irradiated calorimeter cell (A13) decreased by approximately 16% (approximately 8% due to scintillator degradation and 8% due to PMTs response loss) during the Run-2 (Figure 5b) [6].

3.6 Time calibration

Since the correct energy reconstruction of the OF algorithm depends on the precise knowledge of the time phase of the signal with respect to the LHC clock, the time setting of each TileCal channel is adjusted so that the particles traveling at the speed of light that originated from the ATLAS interaction point generate a signal pulse with the time phase equal to zero. Besides the energy reconstruction, time calibration is also important for non-collision background removal and time-of-flight measurements.

The time calibration is performed using multiple types of data (laser system, beam-splash events, ...), the final of which uses *pp* collision data [6]. To mitigate the pile-up noise and non-collision background, in each event, only channels that belong to the reconstructed jets are

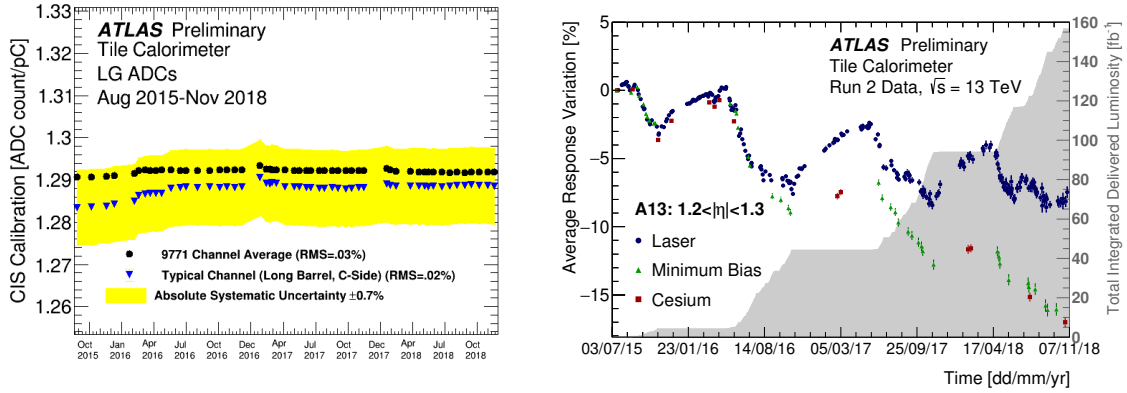

(a) **(b)**

Figure 5: (a) LG CIS calibration constants as a function of time during Run-2 [4]. (b) Variation of the response to the (blue) laser, (green) MB, and (red) cesium systems in Run-2 for cell A13 [4].

considered. Since the reconstructed time of jets slightly depends on the measured cell energy (Section 4.3), additional cut 2 GeV $< E_{\text{channel}} <$ 4 GeV is used for HG and 15 GeV $< E_{\text{channel}} <$ 50 GeV for LG [6]. The average channel time in both gains is used to adjust the corresponding time constants.

To monitor the time calibration and to correct for the timing instabilities (like timing jumps, more in [6]), two methods are used. First, the laser events are recorded during empty LHC bunch crossings during physics data taking. As a result, reconstructed time as a function of luminosity block [6] is obtained in each channel (Figure 6a). Second, the jets from physics data are used to obtain the average reconstructed time in each channel (Figure 6b).

4. Performance

4.1 Response to single muons

To validate the calorimeter response on the electromagnetic scale and to check the response uniformity, events with single isolated muons are used. Muons considered in this analysis (more in [6]) originate from the decay of W bosons ($W \to \mu\nu$) produced in the pp collisions. To probe the cell response, the truncated mean $\langle \Delta E/\Delta x \rangle_{1\%}$ of the muon energy loss ΔE per unit distance Δx (omitting 1% of the events with the largest $\Delta E/\Delta x$ values) of data is compared to the Monte Carlo simulation:

$$R = \frac{\langle \Delta E/\Delta x \rangle_{1\%}^{\text{data}}}{\langle \Delta E/\Delta x \rangle_{1\%}^{\text{MC}}}.$$

The ratio R (Figure 7a) is close to unity for all standard calorimeter cells, validating the calorimeter response on the electromagnetic scale. The average non-uniformity of cells across the calorimeter modules is 2.4% [6].

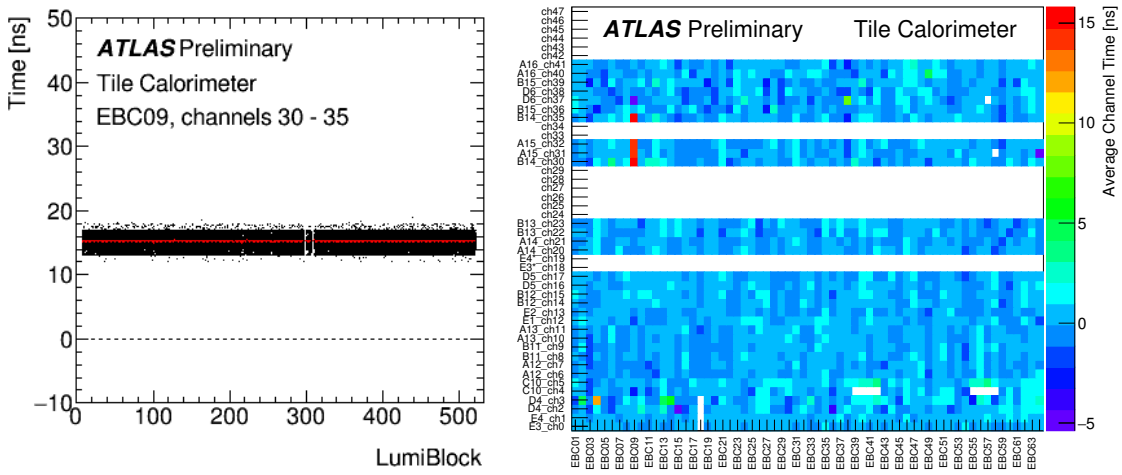

(a) **(b)**

Figure 6: (a) Reconstructed time as a function of luminosity block using laser events [4]. (b) Average reconstructed time as a function of module and channel numbers using physics data [9]. Both time monitoring methods simultaneously observe a timing jump of approximately 15 ns.

4.2 Response to single hadrons

Response of the calorimeter is also probed using single hadrons originating from pp collisions with a low average number of interactions per bunch crossing (more in [6]). The ratio E/p of the energy E measured by the calorimeter to the corresponding momentum p measured by the ATLAS Inner Detector is used. Due to the non-compensating character of the calorimeter, the ratio E/p is approximately 60% and shows dependence on the jet momentum (Figure 7b) and pseudorapidity [6].

4.3 Time performance

Time performance is studied using collision data utilizing calorimeter cells that belong to the reconstructed jets. Events are separated into bins based on the measured cell energy E_{cell}. In each bin, the core of the reconstructed time distribution is fitted by the Gaussian function and the Gaussian width σ is used as the time resolution. A slight dependence of the mean time on the cell energy is observed due to the slow hadronic component of hadronic showers (Figure 8a). The time resolution is better than 1 ns for $E_{\text{cell}} > 4$ GeV in the long barrel and approaches 0.4 ns (Figure 8b). The resolution is systematically worse in the extended barrel due to larger cells.

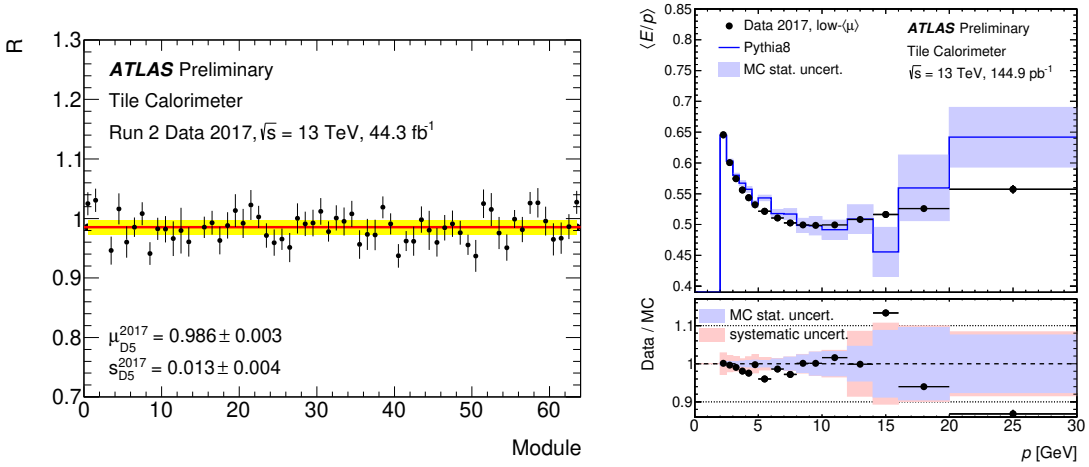

(a) **(b)**

Figure 7: (a) Ratio of data to simulation R of isolated muon energy loss per unit distance as a function of module number for one of the calorimeter cell types [9]. (b) Calorimeter response to isolated charged hadrons as a function of momentum p [9].

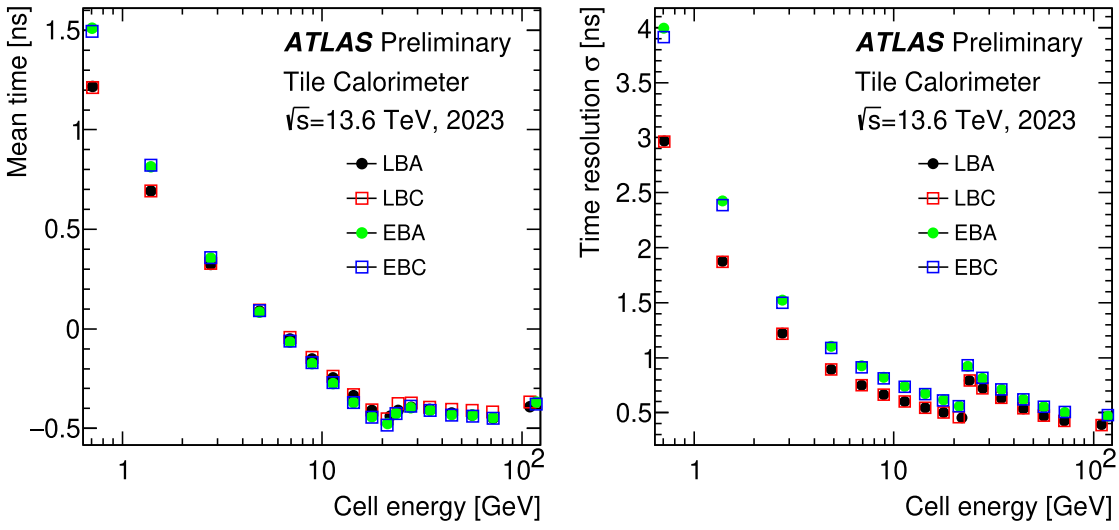

(a) **(b)**

Figure 8: (a) The mean cell time and (b) time resolution as a function of the cell energy using jets in 2023 physics data for the partitions of the long barrel (LBA, LBC) and extended barrel (EBA, EBC) [9].

5. Summary

The ATLAS Tile Calorimeter uses multiple calibration systems to calibrate and monitor each stage of the signal production. Each system has a precision better than approximately 1%.

The energy response of TileCal was validated and studied using isolated muons and hadrons, showing good uniformity and stability.

The timing performance was studied using collision data. The time resolution of TileCal is better than 1 ns for energy larger than few GeV deposited in a single cell.

References

[1] ATLAS Collaboration, *The ATLAS Experiment at the CERN Large Hadron Collider*, *JINST* **3** (2008) S08003.

[2] L. Evans and P. Bryant, *LHC Machine*, *JINST* **3** (2008) S08001.

[3] ATLAS Collaboration, *ATLAS Tile Calorimeter: Technical Design Report*, ATLAS-TDR-3; CERN-LHCC-96-042 (1996).

[4] ATLAS Collaboration, *Approved Tile Calorimeter Plots*, https://twiki.cern.ch/twiki/bin/view/AtlasPublic/ApprovedPlotsTile.

[5] ATLAS Collaboration, *Operation and performance of the ATLAS Tile Calorimeter in Run 1*, *Eur. Phys. J. C* **78** (2018) 987 [1806.02129].

[6] ATLAS Collaboration, *Operation and performance of the ATLAS tile calorimeter in LHC Run 2*, 2401.16034.

[7] ATLAS Collaboration, *Testbeam studies of production modules of the ATLAS tile calorimeter*, *Nucl. Instrum. Meth. A* **606** (2009) 362.

[8] ATLAS Collaboration, *Laser calibration of the ATLAS Tile Calorimeter during LHC Run 2*, *JINST* **18** (2023) P06023 [2303.00121].

[9] ATLAS Collaboration, *Public Tile Calorimeter Plots for Collision Data*, https://twiki.cern.ch/twiki/bin/view/AtlasPublic/TileCaloPublicResults.